HHS Public Access

Author manuscript

Mol Reprod Dev. Author manuscript; available in PMC 2024 February 01.

Published in final edited form as:

Mol Reprod Dev. 2023 February ; 90(2): 98–108. doi:10.1002/mrd.23663.

Early embryonic lethality of mice lacking POLD2

Xiaoqing Wu[a,#], **Yong Liu**[a,b,#,*], **Wenying Wang**[a], **Kate Crimmings**[b], **Andrea Williams**[b], **Jesse Mager**[b,*], **Wei Cui**[b,c,*]

[a]Anhui Province Key Laboratory of Embryo Development and Reproductive Regulation, Anhui Province Key Laboratory of Environmental Hormone and Reproduction, Fuyang Normal University, Fuyang, Anhui, China

[b]Department of Veterinary and Animal Sciences, University of Massachusetts, Amherst, MA, USA

[c]Animal Models Core Facility, Institute for Applied Life Sciences (IALS), University of Massachusetts, Amherst, MA, USA

Abstract

As a highly conserved DNA polymerase (Pol), Pol δ plays crucial roles in chromosomal DNA synthesis and various DNA repair pathways. However, the function of POLD2, the second small subunit of DNA Pol δ (p50 subunit), has not been characterized *in vivo* during mammalian development. Here, we report for the first time, the essential role of subunit POLD2 during early murine embryogenesis. Although *Pold2* mutant mouse embryos exhibit normal morphology at E3.5 blastocyst stage, they cannot be recovered at gastrulation stages. Outgrowth assays reveal that mutant blastocysts cannot hatch from the zona pellucida, indicating impaired blastocyst function. Notably, these phenotypes can be recapitulated by siRNA-mediated knockdown, which also exhibit slowed cellular proliferation together with skewed primitive endoderm and epiblast allocation during the second cell lineage specification. In summary, our study demonstrates that POLD2 is essential for the earliest steps of mammalian development, and the retarded proliferation and embryogenesis may also alter the following cell lineage specifications in the mouse blastocyst embryos.

Keywords

Preimplantation embryo; Inner cell mass; Cell lineage specification; Knockout allele; siRNA knockdown

Introduction

Mammalian preimplantation embryo development refers to the time window that starts from oocyte fertilization and concludes with the formation of a blastocyst (Arny et al.

[*]Corresponding author: Department of Veterinary and Animal Sciences, University of Massachusetts, Amherst, MA 01003, USA, liuyong@fynu.edu.cn (Y. Liu), jmager@umass.edu (J. Mager), wcui@umass.edu (W. Cui).
[#]Equal contribution

Declaration of interest

The authors declare that there is no conflict of interest that could be perceived as prejudicing the impartiality of the research reported.

1987). To form a competent blastocyst that is capable of uterine implantation, three major transcriptional and morphogenic events must occur. The first event, maternal-to-zygotic transition (MZT), initiates the degradation of maternal mRNAs and proteins with replacement from zygotic transcripts to establish totipotency (Latham et al. 1991, Liu et al. 2018). Upon reaching 8-cell stage in the mouse, embryo initiates compaction and polarization, events critical for the first cell-fate acquisition (Houliston and Maro 1989, Sutherland and Calarco-Gillam 1983). Following this, the last major preimplantation event occurs, which is blastomere cell fate allocation resulting in the outer polar cells differentiating exclusively into the trophectoderm (TE), whereas the apolar cells located inside of the morula give rise to the inner cell mass (ICM) (Hogan and Tilly 1978). In the mouse, when blastocysts reach 32–64 cell stage, the ICM segregates into the pluripotent epiblast (EPI) lineage and the primitive endoderm (PE) lineage (Gardner 1982). These first three lineages (EPI, PE, and TE) will give rise to the embryo, parietal yolk sac, and placenta, respectively (Frum and Ralston 2015, Marikawa and Alarcon 2009).

Expression of more than 11,000 genes has been detected during mammalian preimplantation development (Xue et al. 2013), and numerous studies have suggested that early embryogenesis is a highly regulated process that relies on the differential expression of various genes among different stages and distinct cell populations. For example, in the mouse, the transcription factor (TF) CDX2 becomes exclusively expressed in TE, whereas the TF OCT4 (alias POU5F1) becomes highly expressed in the ICM (Niwa et al. 2005) during the first cell fate determination. Similarly, the segregation of EPI and PE lineages within the ICM is demarcated by NANOG expression in EPI lineage and SOX17 in the PE (Artus et al. 2011, Frum et al. 2019). Through advances in gene editing and loss-of-function studies, increasing numbers of genes and factors have been proven to be essential during early lineage specification in mammalian embryos. For example, members of Hippo signaling pathway (Nishioka et al. 2009, Strumpf et al. 2005, Wicklow et al. 2014, Yagi et al. 2007), Notch signaling (Rayon et al. 2014), WNT signaling (Denicol et al. 2014), and ROCK signaling (Kono et al. 2014, Negron-Perez et al. 2018) have all been implicated in normal development. Furthermore, epigenetic regulation (Chen et al. 2016, Chung et al. 2017, Li et al. 2019, Marcho et al. 2015) and newly discovered factors, such as NOP2 (Cui et al. 2016b, Wang et al. 2020), SBNO1 (Watanabe et al. 2017), TFAP2C (Cao et al. 2015), SMCHD1 (Midic et al. 2018, Schall et al. 2019), and RBBP4 (Miao et al. 2020a, Zhao et al. 2020), also contribute to and dictate these unique cellular identities whose proper development are essential for further embryogenesis. Notably, our recent study on MED20 suggests that the Mediator complex, which was considered a basic part of universal RNA polymerase (Pol) II transcription machinery for all genes, interacts with specific TFs and co-factors to ensure certain genes are expressed within different cell populations (Cui et al. 2019).

Another evolutionarily conserved multi-subunit complex involved during mammalian embryogenesis is DNA Polymerase. Among multiple DNA Pol members, highly conserved Pol δ plays crucial roles in chromosomal DNA synthesis, DNA repair, genome maintenance, and 3’ to 5’ exonuclease activity (Prindle and Loeb 2012). DNA Pol δ was originally characterized as a heterodimer composed of two subunits p125 and p50, after which, another two subunits p68 and p12 were also identified (Hindges and Hubscher 1997, Xie et al. 2002,

Zhang et al. 1995). Among these four subunits, the catalytic subunit p50 (also known as POLD2) serves as a scaffold for the assembly of Pol δ by interacting simultaneously with each of the other three subunits (Baldeck et al. 2015). Given its core function in Pol δ and DNA replication, POLD2 has been reported to be a potential prognostic biomarker in several types of carcinomas, where high levels of POLD2 are associated with malignancy and poor survival (Elgaaen et al. 2010, Xu et al. 2020). Interestingly, a recent study in plant Arabidopsis found that POLD2, in addition to maintaining genomic stability, can also participate in the regulation of gene expression through interactions with epigenetic machinery although the detailed mechanisms are still largely unknown (Zhang et al. 2016). To date, the function of POLD2 has not been characterized *in vivo* by knockout (KO) or *in vitro* by knockdown (KD) during mammalian embryogenesis.

In the present study, we use both KO and KD strategies to explore the role of POLD2 during murine development. Our data suggest that POLD2 is essential for early embryogenesis and successful implantation due to its indispensable functions in cell proliferation.

2. Material and methods

Unless otherwise specified, all chemicals and media were obtained from Millipore-Sigma (Burlington, MA, USA).

2.1 Generation of *Pold2* mutants

All animal experimental protocols were approved by the Institutional Animal Care and Use Committee of the University of Massachusetts, Amherst (2015–0011, 2018–0003). *Pold2* KO allele (C57BL/6N-*Pold2*$^{tm1.1(KOMP)Vlcg}$/JMmucd, Stock#: 049145-UCD) was generated on C57BL/6N background by the Knockout Mouse Phenotyping Program (KOMP2) at The Jackson Laboratory (JAX). Briefly, a beta-galactosidase containing ZEN-UB1 Velocigene cassette (Cassette#: 13729) was inserted into the *Pold2* gene, replacing all coding exons (except the first ATG) and intervening sequences (Fig. 1A) and creating a deletion of 4,772 bp between positions 5,876,929 – 5,872,158 of Chromosome 11 (Genome Build 38). The construct was introduced into C57BL/6N-derived VGB6 embryonic stem cells and the resulting chimeras were mated to C57BL/6N mice. Heterozygous offspring were crossed to a ubiquitous Cre deleter mouse line B6N.Cg-Tg(Sox2-cre)1Amc/J for recombination of the LoxP sites to remove the neo cassette and the offspring that didn't contain the *Cre* transgene were maintained for colony establishment. To expand the mouse line in our lab, heterozygous (Het) mice from JAX were backcrossed again with C57BL/6N wildtype (WT). Heterozygous intercrosses were used to generate *Pold2* mutants (Mut). The genotyping primers include: WT Forward: CCGGTATAGCAGCATGGAAG; WT Reverse: TCTCACTGAATGCCAACAGC; Mut Forward: CGGTCGCTACCATTACCAGT; Mut Reverse: AAGGAAGCCAACGTCACATC.

2.2 Embryo recovery, culture and genotyping

For natural matings, *Pold2* heterozygous females 8- to 14-weeks old were caged with *Pold2* heterozygous males and the presence of a vaginal plug was defined as embryonic day 0.5 (E0.5). Embryos were collected from heterozygous females by dissection or flushing to

collect E7.5 or E3.5 embryos, respectively. Embryos were imaged, collected into individual tubes and then lysed for PCR genotyping as previously described (Miao et al. 2020b).

To prepare zygotes for siRNA microinjection and *in vitro* culture and immunofluorescence, B6D2F1 female mice 8- to 10-weeks old were super-ovulated with 10 IU pregnant mare serum gonadotropin (PMSG, BioVendor, Asheville, NC, USA), followed 48 hr later by 10 IU human chorionic gonadotropin (hCG). Females were then mated with B6D2F1 males and euthanized 20 hr post-hCG injection. Zygotes were released from oviducts in M2 medium (MR015D), and cumulus cells were removed in hyaluronidase medium (MR051F) as described previously (Miao and Cui 2022). Zygotes were washed in M2 and cultured in KSOM at 37 °C in a humidified atmosphere of 5% CO_2, 5% O_2 balanced in N_2.

2.3 Outgrowth assay

Blastocysts were harvested and cultured individually in a single well of DMEM (Lonza, Allendale, NJ, USA) containing 10% fetal bovine serum (FBS, Atlanta Biologicals, Flowery Branch, GA, USA) and 1X GlutaMAX (Thermo Fisher Scientific, Waltham, MA, USA). Blastocysts were allowed to attach and outgrow for 3 days at 37 °C in a humidified atmosphere of 5% CO_2 prior to imaging and genotyping. Outgrowths were evaluated by morphology as demonstrated before (Cui et al. 2016a). Briefly, embryonic outgrowth that displays a distinctive ICM colony surrounded by a trophoblast monolayer is considered normal outgrowth, while embryos that could not hatch or outgrowths that lack ICM colony or trophoblast monolayer are considered failed.

2.4 Immunofluorescence and imaging of preimplantation embryos

Immunofluorescence (IF) was performed as previously described (Su et al. 2021). After siRNA microinjection, injected zygotes were cultured for 4 days to reach blastocyst stage. Blastocysts were fixed in 4% paraformaldehyde and briefly washed in PBS, followed by permeabilization with 0.5% Triton X-100 in PBS for 20 min. Embryos were then blocked in blocking solution (PBS with 10% FBS and 0.1% Triton) for 1 h at room temperature, and then incubated with primary antibodies overnight at 4 °C. All primary antibodies were diluted 1:200 using the blocking solution, including: mouse anti-CDX2 (BioGenex, MU392A-UC); rabbit anti-NANOG (abcam, ab80892); rabbit anti-TRP53 (Cell Signaling Technology, #9284); rabbit anti-POLD2 (Invitrogen, PA5–55401); goat anti-SOX17 (R&D Systems, AF1924); goat anti-OCT4 (abcam, ab27985). After suitable secondary antibody (Donkey anti-Goat 488, A32814; Donkey anti-Rabbit 546, A10040; Donkey anti-Mouse 647, A31571, Alexa Fluor, Thermo Fisher Scientific, Waltham, MA, USA) and DAPI staining, embryos were mounted and imaged under a Nikon A1 Spectral Detector Confocal with FLIM Module. Z-stacks (20X objective, 8 μm sections) were collected and maximum projection applied. Fluorescence intensity was quantified and analyzed as described (Su et al. 2021). Briefly, all high-resolution z-stack images were acquired under identical settings, and relative intensities were measured on the raw images using ImageJ software (Schneider et al. 2012) under fixed thresholds and parameters across all slides, with DAPI intensity as the reference.

2.5 X-gal (5-bromo-4-chloro-3-indolyl-β-D-galactopyranoside) staining

Freshly dissected embryos were fixed in X-gal buffer containing 0.2% glutaraldehyde and 1% formaldehyde on ice for 15 min and subjected to modifications from the previous protocol (Cui et al. 2020, Tremblay et al. 2000). In brief, the fixed embryos were washed with X-gal buffer (PBS, 5 mM EGTA, 2 mM MgCl:6H2O, 0.2% NP-40, 0.2 mM deoxycholate) for 10 min three times, and stained with X-gal stain (X-gal buffer with 5mM potassium ferricyanide, 5mM potassium ferrocyanide, and 0.5 mg/ml X-gal) for 48 hours at 37°C. Subsequently, embryos were dehydrated in ethanol, cleared in xylene, embedded in paraffin, and sectioned at 7 μm. Slides were deparaffinated in xylene, counterstained with Eosin and coverslipped in Cytoseal (Thermo Fisher Scientific, Waltham, MA, USA) and imaged with a Pannoramic MIDI II slide scanner (3DHISTECH Ltd., Budapest, Hungary).

2.6 Microinjection

Microinjection was performed as previously described (Cui et al. 2016a). A volume of 5–10 pl of 50 μM Scrambled Control (5'-UUCUCCGAACGUGUCACGU) or *Pold2* siRNA (5'-GCAACCUGCUCAGCCAUAA, Genepharma, China) was microinjected into the cytoplasm of zygotes.

2.7 RNA extraction and quantitative real-time PCR (qPCR)

Total RNA was extracted from different stages of oocytes and embryos (20 oocytes or embryos per stage during each replicate) using the Roche High Pure RNA Isolation Kit (#11828665001), and cDNA was synthesized using iScript cDNA synthesis kit (#170–8891, Bio-Rad Laboratories, CA, USA). All qPCR reactions were performed on the CFX96 Touch™ Real-Time PCR Detection System (Bio-Rad Laboratories, CA, USA) and the intron-spanning primers used for qPCRs are as follows: *Pold2*, 5'-CAGCCATAACACCCAGAGCA and 5'-AGGCACTCAGTTGCAGAAGG; *Gapdh*, 5'-TCAACAGCAACTCCCACTCTTCCA and 5'-ACCCTGTTGCTGTAGCCGTATTCA. Transcripts of examined genes were quantified in triplicates and calculated relative to the transcription of the housekeeping gene *Gapdh*. The specificity of the qPCR reaction was confirmed by both single peaks in the melt curves and gel electrophoresis. Similarly, for KD validation, embryos at the morula stage and blastocyst stage (2.5 and 3.5 days after microinjection, respectively) were lysed (15 embryos per stage in each replicate) for RNA extraction and qPCR with 3 replicates total.

2.8 Statistical Analysis

All experiments were repeated at least three times. Percentage data were analyzed by ANOVA, and a value of $P < 0.05$ was considered statistically significant. Data are expressed as mean ± standard error of the mean. The number of embryos used in each experiment was listed either in the Results section or in the figure legends.

3. Results

3.1 *Pold2* mutants cannot be recovered *in vivo* after E3.5

The *Pold2* knock-out allele was generated by insertion of ZEN-UB1 Velocigene cassette (Cassette#: 13729, http://velocigene.com/komp/detail/13729#clones) for the Knockout Mouse Phenotyping Program (KOMP2) at The Jackson Laboratory (Fig. 1A). During the initial phenotyping performed for the International Mouse Phenotyping Consortium (IMPC, https://www.mousephenotype.org), no homozygous *Pold2* mutants were born, nor found at E15.5 or E12.5 (WT=44, Het=86, Mut=0). Therefore, we first dissected embryos at E7.5. Twenty-two E7.5 embryos were recovered from 4 heterozygous intercrosses. Genotyping revealed that we recovered 12 Het and 10 WT embryos (Fig. 1B). No *Pold2* homozygous mutant embryos were present at E7.5. However, there was an obviously increased number of empty decidua (n = 18), suggesting that *Pold2* mutants may trigger decidual response but do not produce viable gastrulation stage embryos. To gain more insight into the mechanism underlying the embryonic lethality in vivo, we collected E3.5 blastocysts for morphological assessment. From 6 litters of embryos at E3.5, we recovered 8 *Pold2* mutants, 15 Het and 10 WT embryos at the blastocyst stage. Mutant blastocysts were indistinguishable from littermates based on morphology alone (Fig. 1C). Therefore, we further tested by performing a 3-day-outgrowth assay as surrogate for implantation. The majority of WT (66.7%, 2/3) and Het blastocysts (75%, 6/8) showed successful outgrowths displaying distinct 3-dimensional ICM colonies surrounded by adherent trophoblast cells. However, none of the 5 mutants (0%, 0/5) formed a successful outgrowth failing to hatch from the zona pellucida (Fig. 1D). These results are consistent with a complete absence of mutant embryos at E7.5.

3.2 Expression of POLD2 during early mouse embryogenesis

Based on the phenotype and timing of lethality, we evaluated POLD2 expression during preimplantation and gastrulation stages. Immunofluorescence (IF) and RT-PCR analysis of WT preimplantation embryos revealed that *Pold2* mRNA and protein are present at all stages examined (Fig. 2A, B, C). Interestingly, the highest mRNA was detected at MII stage (Fig. 2A), suggesting post-transcriptional modification(s) may occur after GV stage since fully grown GV oocytes normally are transcriptionally silent. POLD2 protein is concentrated in the nucleus from GV stage oocytes through the blastocyst stage, except MII oocytes (Fig. 2C). Notably, POLD2 protein is present in all cells at blastocyst stage, without obvious difference among distinct cell lineages (EPI, PE, and TE). We also examined *Pold2* expression during gastrulation by examining expression of the *LacZ* reporter, inserted during generation of the knock-out allele, in Het embryos. Interestingly, at E7.5, LacZ is detected in ectoderm and mesoderm (including extra-embryonic mesoderm) but is largely absent from the definitive endoderm and visceral endoderm (Fig. 2D). At E8.5, this pattern continues but with LacZ enriched in head fold and heart (Fig. 2E). Together, although POLD2 is present at all stages and cell lineages during preimplantation development, its expression becomes distinct and divergent among the embryonic lineage derivatives and specific organ precursors during gastrulation stages.

3.3 *Pold2* knockdown embryos phenocopy genetic mutants

In order to establish a more efficient platform for studying the function of POLD2 during development, we used RNA interference (RNAi) to knockdown (KD) *Pold2*. Either scrambled control siRNA or *Pold2*-siRNA was microinjected into mouse zygotes and after microinjection, embryos were cultured to different stages. Robust KD efficacy was confirmed by qPCR at the morula and blastocyst stages (Fig. 3A). KD efficacy was also determined by POLD2 IF at blastocyst stage (Fig. 3B), further validating the specificity of the antibody used in the present study. Similar to the KO phenotype, *Pold2* KD did not affect blastocyst morphology or formation (Fig 3C, D) but did lead to outgrowth failure when KD embryos were subjected to the 72-hour outgrowth assay (Fig 3E, F). These results suggest that the phenotypes of *Pold2* KOs can be recapitulated by microinjection of *Pold2* siRNA, resulting in outgrowth failure in the absence of POLD2 function.

3.4 POLD2 deficiency does not alter ICM/TE specification

To explore the mechanism of embryonic lethality *in vivo* and outgrowth failure *in vitro*, we first examined markers of apoptosis (Ser15-phospho active TRP53) and the first cell lineage specification (OCT4 for ICM and CDX2 for TE). As shown in figure 4A, both control and KD embryos have no obvious apoptosis, with normal robust expression of OCT4 in ICM and mutually exclusive expression of CDX2 in TE. Although the numbers of both OCT4 positive cells (Fig 4B) and CDX2 positive cells (Fig 4C) were significantly decreased in KD group, the total cell number is also significantly reduced in KD blastocysts (Fig 4D). However, the percentages of OCT4 (Fig 4E) and CDX2 (Fig 4F) positive cells are not different in KD embryos, indicating that POLD2 may alter cell proliferation rates, but not ICM/TE specification during the first cell lineage segregation.

3.5 *Pold2* KD embryos have defective PE/EPI allocation.

We then investigated the fidelity of the second embryonic lineage specification, the allocation of primitive endoderm (PE) and epiblast (EPI) from the ICM by assessing the PE marker SOX17 and the EPI marker NANOG (Fig. 5A). As shown in Fig. 5B and C, KD blastocysts contained a significantly reduced number of PE cells (SOX17 positive), but no obvious change was detected in the number of EPI cells (NANOG positive) when compared with control embryos. Intriguingly, the percentage of PE cells is decreased (Fig. 5F) while the percentage of EPI cells is increased (Fig. 5G), suggesting PE/EPI allocation within ICM was altered in *Pold2* KD blastocysts. However, whether the skewed PE/EPI allocation is a direct consequence of POLD2 reduction or just an accompanying result of slowed embryogenesis with fewer total cell numbers, requires further investigation.

Discussion

Early embryogenesis is a highly regulated process comprised of highly regulated cellular events, including proliferation and differentiation. Given the essential role of POLD2 (catalytic subunit p50) in the assembly of Pol δ, a highly conserved DNA Pol member with crucial roles during DNA synthesis and genome maintenance (Baldeck et al. 2015), it is not surprising that POLD2 has been reported as a biomarker of tumorigenesis and malignancy (Elgaaen et al. 2010, Xu et al. 2020). Here we show for the first time that POLD2 is essential

during early mammalian development. Although the morphology of mutant blastocysts (either genetic mutants or siRNA-KD) is indistinguishable from the control embryos, IF and cell counting indicate a significant decrease of total cell number at the blastocyst stage, suggesting a function of POLD2 in regulating cell proliferation during early mammalian embryogenesis. This may also explain, at least partially, the outgrowth failure observed in *Pold2* KO and KD embryos. Also, outgrowth failure clearly explains the lack of mutant embryos found at gastrulation stages.

In addition to cell proliferation, we also tested cell differentiation and lineage specification, a major challenge relying on the differential expression of various genes among distinct cell populations during embryogenesis. Multiple signaling pathways have been revealed during embryonic lineage specification, such as Hippo signaling in TE (Nishioka et al. 2009) and ICM (Wicklow et al. 2014) specification, Notch (Rayon et al. 2014) and ROCK signaling (Kono et al. 2014, Negron-Perez et al. 2018) in TE fate acquisition, as well as FGF signaling in PE/EPI segregation (Morris et al. 2013, Yamanaka et al. 2010). Although the localization of specific TFs and markers within distinct lineages have been well studied, the upstream regulation of these critical factors is not fully understood (Cui and Mager 2018, Paul and Knott 2014). With advances in genome manipulation, single-cell transcriptomics, and loss-of-function studies, increasing numbers of genes have been revealed as essential during early lineage specification in mammalian embryos. For example, our recent studies demonstrated that both PE and EPI were altered in *Rbbp4* mutant embryos (Miao et al. 2020a), whereas only EPI but not PE was affected in *Mcrs1* mutants (Cui et al. 2020). Our present study demonstrates skewed PE/EPI allocation in the *Pold2* KD blastocysts, where the percentage of PE and EPI was significantly downregulated and upregulated, respectively. This intriguing phenotype may suggest certain DNA replication factors, such as POLD2, might participate in regulating the expression of genes. However, based on the experiments and the data presented here, it is not adequate to claim POLD2 as a transcription factor or transcription factor regulator since the skewed PE/EPI allocation may be just an accompanying result of slowed embryogenesis with fewer total cell numbers. To test if POLD2 may be required for PE cells and compensated by a different DNA Pol subunit in EPI cells resulting in the lineage-specific differential effects, in vitro culture of blastocysts beyond the implantation stages (Bedzhov et al. 2014) would provide more insights into the underlying mechanisms. Interestingly, a recent study in Arabidopsis indeed found that POLD2 is involved in regulating the bivalent histone modifications, such as H3K27me3 and H3K4me3, during plant cell differentiation and cell-type transition, although the detailed mechanisms are still unknown (Zhang et al. 2016).

Notably, our recent study on Mediator complex, which was considered a basic part of universal RNA Pol II transcription machinery for all genes, suggests that certain Mediator subunits may exert selective affinity among different activators and TFs to ensure certain genes are expressed within different cell populations (Cui et al. 2019). To fully understand the mechanism and specificity of POLD2 function during embryogenesis and lineage specification, further experiments are needed, such as transcriptome wide analysis in KO or KD embryos, and conditional deletion experiments to determine if there are lineage specific requirements of POLD2. Alternatively, different types of blastocyst-derived stem cells (such as ESCs, trophoblast stem cells, and extra-embryonic endoderm cells) may serve as good

models to determine if POLD2 functions differentially with distinct TFs in different cell lineages. It may also be of interest to dissect the different roles of each Pol δ subunit during embryo development, where loss of either *Pold2* (our present study) or *Pold3* (Zhou et al. 2018) causes peri-implantation lethality while loss of *Pold1* (http://www.informatics.jax.org/marker/MGI:97741) or *Pold4* (https://www.mousephenotype.org/data/genes/MGI:1916995) exhibits no obvious change during murine embryogenesis.

In summary, our data suggest that POLD2 plays a significant role in cell proliferation during mouse preimplantation development required for successful hatching, implantation, and further embryogenesis.

Acknowledgments

The authors thank the Knockout Mouse Phenotyping Program (KOMP2) and The Jackson Laboratory for providing *Pold2*-knockout allele. This work was supported by the faculty start-up fund and USDA National Institute of Food and Agriculture/Hatch (NIFA/Hatch #1024792) to WC, and NIH R01HD083311 to JM. The confocal microscopy data were gathered in the Light Microscopy Facility and Nikon Center of Excellence at the Institute for Applied Life Sciences, UMass Amherst with support from the Massachusetts Life Sciences Center.

Funding information:

Faculty start-up fund; USDA National Institute of Food and Agriculture/Hatch (NIFA/Hatch #1024792); National Institutes of Health (R01HD083311).

References

Arny M, Nachtigall L & Quagliarello J 1987 The effect of preimplantation culture conditions on murine embryo implantation and fetal development. Fertil Steril 48 861–865. [PubMed: 3666190]

Artus J, Piliszek A & Hadjantonakis AK 2011 The primitive endoderm lineage of the mouse blastocyst: sequential transcription factor activation and regulation of differentiation by Sox17. Dev Biol 350 393–404. [PubMed: 21146513]

Baldeck N, Janel-Bintz R, Wagner J, Tissier A, Fuchs RP, Burkovics P, Haracska L, Despras E, Bichara M, Chatton B et al. 2015 FF483–484 motif of human Poleta mediates its interaction with the POLD2 subunit of Poldelta and contributes to DNA damage tolerance. Nucleic Acids Res 43 2116–2125. [PubMed: 25662213]

Bedzhov I, Leung CY, Bialecka M & Zernicka-Goetz M 2014 In vitro culture of mouse blastocysts beyond the implantation stages. Nat Protoc 9 2732–2739. [PubMed: 25356584]

Cao Z, Carey TS, Ganguly A, Wilson CA, Paul S & Knott JG 2015 Transcription factor AP-2gamma induces early Cdx2 expression and represses HIPPO signaling to specify the trophectoderm lineage. Development 142 1606–1615. [PubMed: 25858457]

Chen Z, Hagen DE, Wang J, Elsik CG, Ji T, Siqueira LG, Hansen PJ & Rivera RM 2016 Global assessment of imprinted gene expression in the bovine conceptus by next generation sequencing. Epigenetics 11 501–516. [PubMed: 27245094]

Chung N, Bogliotti YS, Ding W, Vilarino M, Takahashi K, Chitwood JL, Schultz RM & Ross PJ 2017 Active H3K27me3 demethylation by KDM6B is required for normal development of bovine preimplantation embryos. Epigenetics 12 1048–1056. [PubMed: 29160132]

Cui W, Cheong A, Wang Y, Tsuchida Y, Liu Y, Tremblay KD & Mager J 2020 MCRS1 is essential for epiblast development during early mouse embryogenesis. Reproduction 159 1–13. [PubMed: 31671403]

Cui W, Dai X, Marcho C, Han Z, Zhang K, Tremblay KD & Mager J 2016a Towards Functional Annotation of the Preimplantation Transcriptome: An RNAi Screen in Mammalian Embryos. Sci Rep 6 37396. [PubMed: 27869233]

Cui W & Mager J 2018 Transcriptional Regulation and Genes Involved in First Lineage Specification During Preimplantation Development. Adv Anat Embryol Cell Biol 229 31–46. [PubMed: 29177763]

Cui W, Marcho C, Wang Y, Degani R, Golan M, Tremblay KD, Rivera-Perez JA & Mager J 2019 MED20 is essential for early embryogenesis and regulates NANOG expression. Reproduction 157 215–222. [PubMed: 30571656]

Cui W, Pizzollo J, Han Z, Marcho C, Zhang K & Mager J 2016b Nop2 is required for mammalian preimplantation development. Mol Reprod Dev 83 124–131. [PubMed: 26632338]

Denicol AC, Block J, Kelley DE, Pohler KG, Dobbs KB, Mortensen CJ, Ortega MS & Hansen PJ 2014 The WNT signaling antagonist Dickkopf-1 directs lineage commitment and promotes survival of the preimplantation embryo. FASEB J 28 3975–3986. [PubMed: 24858280]

Elgaaen BV, Haug KB, Wang J, Olstad OK, Fortunati D, Onsrud M, Staff AC, Sauer T & Gautvik KM 2010 POLD2 and KSP37 (FGFBP2) correlate strongly with histology, stage and outcome in ovarian carcinomas. PLoS One 5 e13837. [PubMed: 21079801]

Frum T & Ralston A 2015 Cell signaling and transcription factors regulating cell fate during formation of the mouse blastocyst. Trends Genet 31 402–410. [PubMed: 25999217]

Frum T, Watts JL & Ralston A 2019 TEAD4, YAP1 and WWTR1 prevent the premature onset of pluripotency prior to the 16-cell stage. Development 146.

Gardner RL 1982 Investigation of cell lineage and differentiation in the extraembryonic endoderm of the mouse embryo. J Embryol Exp Morphol 68 175–198. [PubMed: 7108421]

Hindges R & Hubscher U 1997 Cloning, chromosomal localization, and interspecies interaction of mouse DNA polymerase delta small subunit (PolD2). Genomics 44 45–51. [PubMed: 9286699]

Hogan B & Tilly R 1978 In vitro development of inner cell masses isolated immunosurgically from mouse blastocysts. II. Inner cell masses from 3.5- to 4.0-day p.c. blastocysts. J Embryol Exp Morphol 45 107–121. [PubMed: 353213]

Houliston E & Maro B 1989 Posttranslational modification of distinct microtubule subpopulations during cell polarization and differentiation in the mouse preimplantation embryo. J Cell Biol 108 543–551. [PubMed: 2645302]

Kono K, Tamashiro DA & Alarcon VB 2014 Inhibition of RHO-ROCK signaling enhances ICM and suppresses TE characteristics through activation of Hippo signaling in the mouse blastocyst. Dev Biol 394 142–155. [PubMed: 24997360]

Latham KE, Solter D & Schultz RM 1991 Activation of a two-cell stage-specific gene following transfer of heterologous nuclei into enucleated mouse embryos. Mol Reprod Dev 30 182–186. [PubMed: 1793594]

Li Y, Hagen DE, Ji T, Bakhtiarizadeh MR, Frederic WM, Traxler EM, Kalish JM & Rivera RM 2019 Altered microRNA expression profiles in large offspring syndrome and Beckwith-Wiedemann syndrome. Epigenetics 14 850–876. [PubMed: 31144574]

Liu Y, Wu F, Zhang L, Wu X, Li D, Xin J, Xie J, Kong F, Wang W, Wu Q et al. 2018 Transcriptional defects and reprogramming barriers in somatic cell nuclear reprogramming as revealed by single-embryo RNA sequencing. BMC Genomics 19 734. [PubMed: 30305014]

Marcho C, Cui W & Mager J 2015 Epigenetic dynamics during preimplantation development. Reproduction 150 R109–120. [PubMed: 26031750]

Marikawa Y & Alarcon VB 2009 Establishment of trophectoderm and inner cell mass lineages in the mouse embryo. Mol Reprod Dev 76 1019–1032. [PubMed: 19479991]

Miao X & Cui W 2022 Berberine alleviates LPS-induced apoptosis, oxidation, and skewed lineages during mouse preimplantation development. Biol Reprod.

Miao X, Sun T, Barletta H, Mager J & Cui W 2020a Loss of RBBP4 results in defective inner cell mass, severe apoptosis, hyperacetylated histones and preimplantation lethality in micedagger. Biol Reprod 103 13–23. [PubMed: 32285100]

Miao X, Sun T, Golan M, Mager J & Cui W 2020b Loss of POLR1D results in embryonic lethality prior to blastocyst formation in mice. Mol Reprod Dev 87 1152–1158. [PubMed: 33022126]

Midic U, Vincent KA, Wang K, Lokken A, Severance AL, Ralston A, Knott JG & Latham KE 2018 Novel key roles for structural maintenance of chromosome flexible domain containing 1 (Smchd1) during preimplantation mouse development. Mol Reprod Dev 85 635–648. [PubMed: 29900695]

Morris SA, Graham SJ, Jedrusik A & Zernicka-Goetz M 2013 The differential response to Fgf signalling in cells internalized at different times influences lineage segregation in preimplantation mouse embryos. Open Biol 3 130104. [PubMed: 24258274]

Negron-Perez VM, Rodrigues LT, Mingoti GZ & Hansen PJ 2018 Role of ROCK signaling in formation of the trophectoderm of the bovine preimplantation embryo. Mol Reprod Dev 85 374–375. [PubMed: 29542836]

Nishioka N, Inoue K, Adachi K, Kiyonari H, Ota M, Ralston A, Yabuta N, Hirahara S, Stephenson RO, Ogonuki N et al. 2009 The Hippo signaling pathway components Lats and Yap pattern Tead4 activity to distinguish mouse trophectoderm from inner cell mass. Dev Cell 16 398–410. [PubMed: 19289085]

Niwa H, Toyooka Y, Shimosato D, Strumpf D, Takahashi K, Yagi R & Rossant J 2005 Interaction between Oct3/4 and Cdx2 determines trophectoderm differentiation. Cell 123 917–929. [PubMed: 16325584]

Paul S & Knott JG 2014 Epigenetic control of cell fate in mouse blastocysts: the role of covalent histone modifications and chromatin remodeling. Mol Reprod Dev 81 171–182. [PubMed: 23893501]

Prindle MJ & Loeb LA 2012 DNA polymerase delta in DNA replication and genome maintenance. Environ Mol Mutagen 53 666–682. [PubMed: 23065663]

Rayon T, Menchero S, Nieto A, Xenopoulos P, Crespo M, Cockburn K, Canon S, Sasaki H, Hadjantonakis AK, de la Pompa JL et al. 2014 Notch and hippo converge on Cdx2 to specify the trophectoderm lineage in the mouse blastocyst. Dev Cell 30 410–422. [PubMed: 25127056]

Schall PZ, Ruebel ML & Latham KE 2019 A New Role for SMCHD1 in Life's Master Switch and Beyond. Trends Genet 35 948–955. [PubMed: 31668908]

Schneider CA, Rasband WS & Eliceiri KW 2012 NIH Image to ImageJ: 25 years of image analysis. Nat Methods 9 671–675. [PubMed: 22930834]

Strumpf D, Mao CA, Yamanaka Y, Ralston A, Chawengsaksophak K, Beck F & Rossant J 2005 Cdx2 is required for correct cell fate specification and differentiation of trophectoderm in the mouse blastocyst. Development 132 2093–2102. [PubMed: 15788452]

Su J, Miao X, Archambault D, Mager J & Cui W 2021 ZC3H4-a novel Cys-Cys-Cys-His-type zinc finger protein-is essential for early embryogenesis in micedagger. Biol Reprod 104 325–335. [PubMed: 33246328]

Sutherland AE & Calarco-Gillam PG 1983 Analysis of compaction in the preimplantation mouse embryo. Dev Biol 100 328–338. [PubMed: 6689157]

Tremblay KD, Hoodless PA, Bikoff EK & Robertson EJ 2000 Formation of the definitive endoderm in mouse is a Smad2-dependent process. Development 127 3079–3090. [PubMed: 10862745]

Wang H, Wang L, Wang Z, Dang Y, Shi Y, Zhao P & Zhang K 2020 The nucleolar protein NOP2 is required for nucleolar maturation and ribosome biogenesis during preimplantation development in mammals. FASEB J 34 2715–2729. [PubMed: 31908012]

Watanabe Y, Miyasaka KY, Kubo A, Kida YS, Nakagawa O, Hirate Y, Sasaki H & Ogura T 2017 Notch and Hippo signaling converge on Strawberry Notch 1 (Sbno1) to synergistically activate Cdx2 during specification of the trophectoderm. Sci Rep 7 46135. [PubMed: 28401892]

Wicklow E, Blij S, Frum T, Hirate Y, Lang RA, Sasaki H & Ralston A 2014 HIPPO pathway members restrict SOX2 to the inner cell mass where it promotes ICM fates in the mouse blastocyst. PLoS Genet 10 e1004618. [PubMed: 25340657]

Xie B, Mazloum N, Liu L, Rahmeh A, Li H & Lee MY 2002 Reconstitution and characterization of the human DNA polymerase delta four-subunit holoenzyme. Biochemistry 41 13133–13142. [PubMed: 12403614]

Xu Q, Hu C, Zhu Y, Wang K, Lal B, Li L, Tang J, Wei S, Huang G, Xia S et al. 2020 ShRNA-based POLD2 expression knockdown sensitizes glioblastoma to DNA-Damaging therapeutics. Cancer Lett 482 126–135. [PubMed: 31954770]

Xue Z, Huang K, Cai C, Cai L, Jiang CY, Feng Y, Liu Z, Zeng Q, Cheng L, Sun YE et al. 2013 Genetic programs in human and mouse early embryos revealed by single-cell RNA sequencing. Nature 500 593–597. [PubMed: 23892778]

Yagi R, Kohn MJ, Karavanova I, Kaneko KJ, Vullhorst D, DePamphilis ML & Buonanno A 2007 Transcription factor TEAD4 specifies the trophectoderm lineage at the beginning of mammalian development. Development 134 3827–3836. [PubMed: 17913785]

Yamanaka Y, Lanner F & Rossant J 2010 FGF signal-dependent segregation of primitive endoderm and epiblast in the mouse blastocyst. Development 137 715–724. [PubMed: 20147376]

Zhang J, Tan CK, McMullen B, Downey KM & So AG 1995 Cloning of the cDNAs for the small subunits of bovine and human DNA polymerase delta and chromosomal location of the human gene (POLD2). Genomics 29 179–186. [PubMed: 8530069]

Zhang J, Xie S, Cheng J, Lai J, Zhu JK & Gong Z 2016 The Second Subunit of DNA Polymerase Delta Is Required for Genomic Stability and Epigenetic Regulation. Plant Physiol 171 1192–1208. [PubMed: 27208288]

Zhao P, Wang H, Wang H, Dang Y, Luo L, Li S, Shi Y, Wang L, Wang S, Mager J et al. 2020 Essential roles of HDAC1 and 2 in lineage development and genome-wide DNA methylation during mouse preimplantation development. Epigenetics 15 369–385. [PubMed: 31533525]

Zhou Z, Wang L, Ge F, Gong P, Wang H, Wang F, Chen L & Liu L 2018 Pold3 is required for genomic stability and telomere integrity in embryonic stem cells and meiosis. Nucleic Acids Res 46 3468–3486. [PubMed: 29447390]

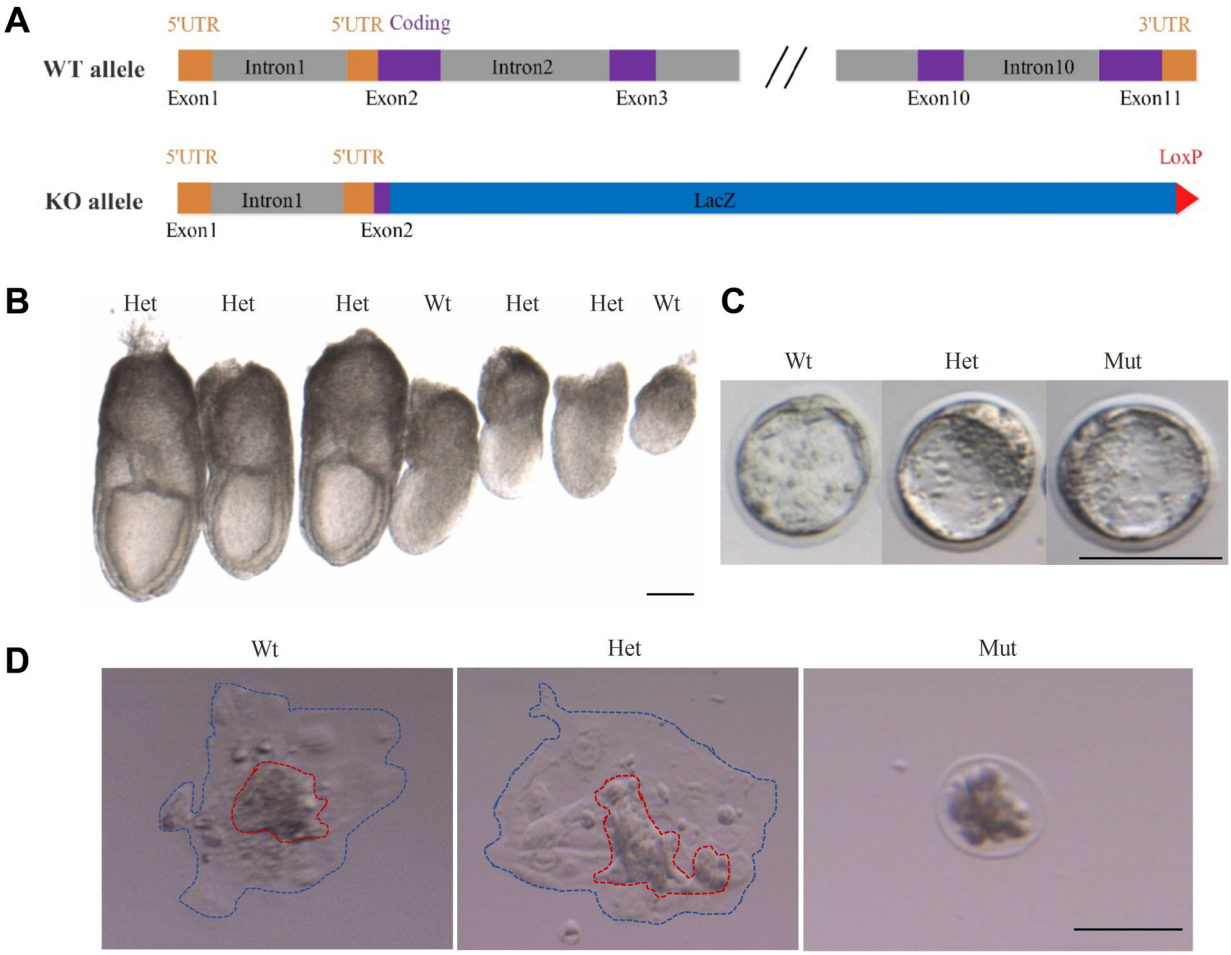

Fig. 1.

Pold2 knock-out allele generation, embryo collection and genotyping, and outgrowth assay. (A) Schematic of *Pold2* knock-out allele generation based on the information provided from IMPC. *lacZ*, β-galactosidase coding sequence from the *E.coli lacZ* gene. (B) Representative genotyped embryos at E7.5 from *Pold2* heterozygous intercrosses. (C) Representative genotyped embryos at E3.5 from *Pold2* heterozygous intercrosses. (D) Outgrowths from WT and Het blastocysts displayed distinctive ICM colonies (red dashed line) surrounded by trophoblast cells (blue dashed line) while all Mut blastocysts could not outgrow. Scale bars, 100 μm.

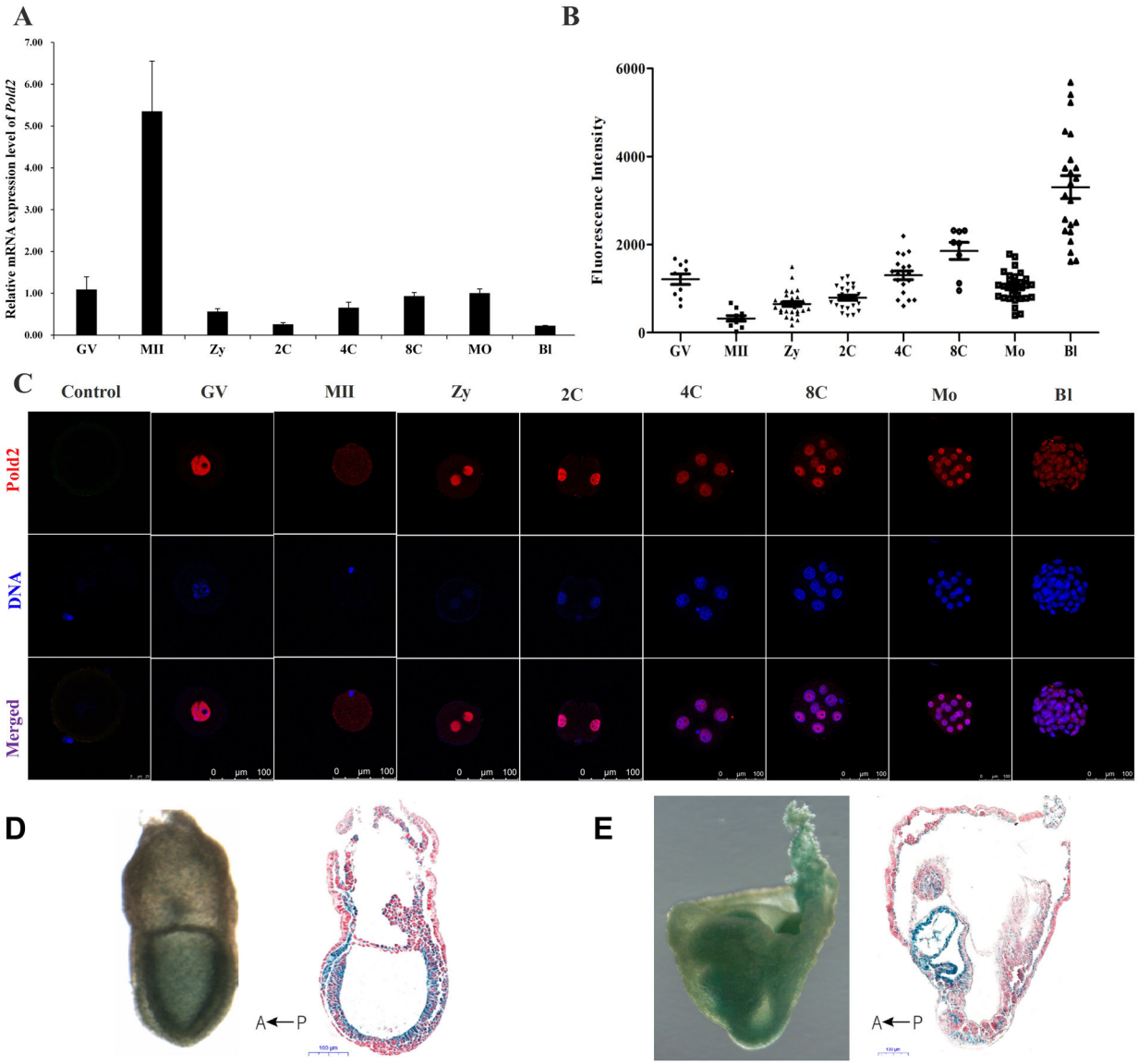

Fig. 2.

Expression of *Pold2* during preimplantation and gastrulation stages. (A) Quantitative real-time PCR (qPCR) to identify *Pold2* expression in WT pre-implantation embryos. *Gapdh* was used as the internal control. (B) Analysis of Immunofluorescence (IF) total intensity per embryo at different stages. Number of samples examined at each stage: GV=10, MII=10, Zy=28, 2C=22, 4C=20, 8C=8, Mo=31, and Bl=22. (C) IF identifying POLD2 protein expression from GV stage oocyte to the blastocyst stage. Control: no primary antibody. (D, E) *LacZ*-reporter staining of both E7.5 (D, n=19) and E8.5 (E, n=8) Het embryos. GV, germinal vesicle stage oocyte; MII, metaphase II oocyte; Zy, zygote; 2/4/8C, 2/4/8 cell stage embryo; Mo, Morula; Bl, Blastocyst; A, anterior; P, posterior.

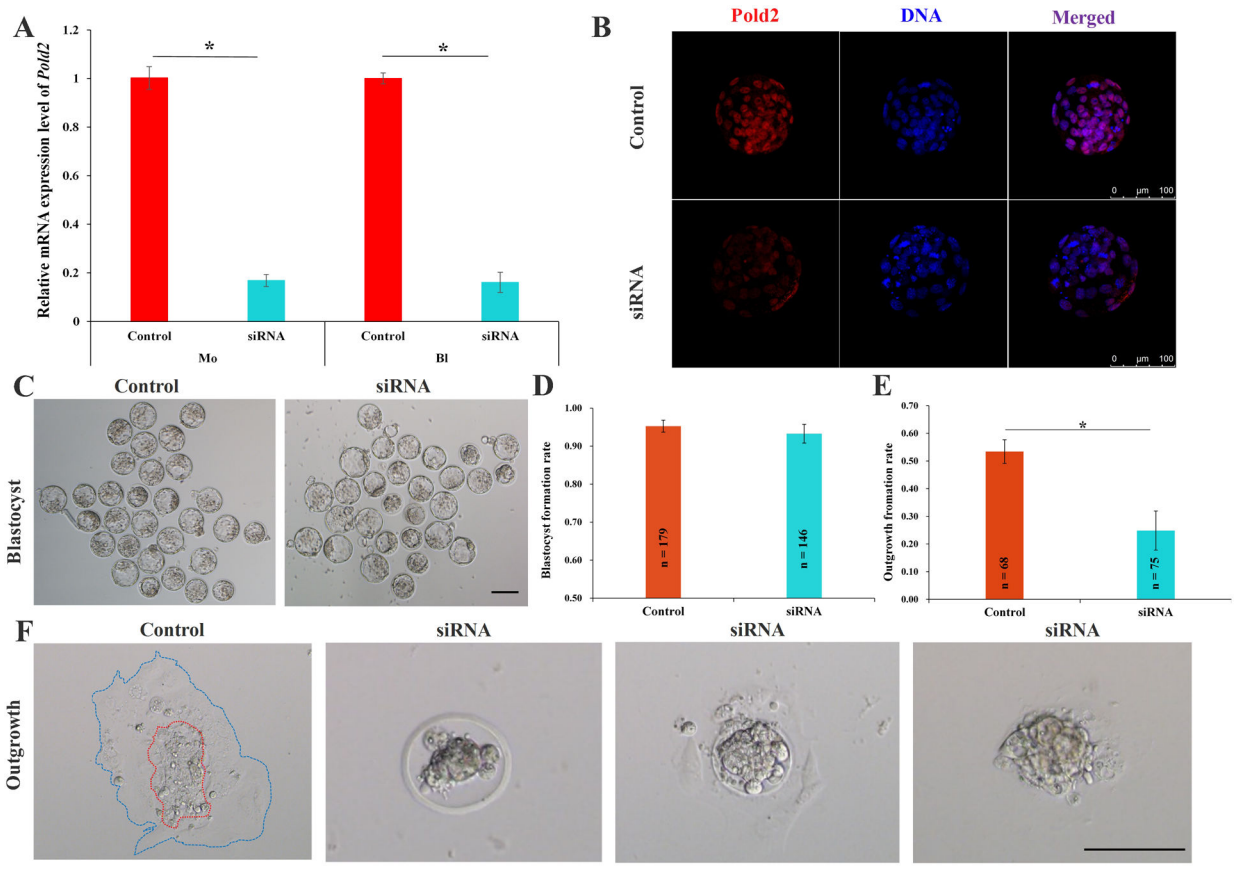

Fig. 3.

Pold2 KD didn't affect blastocyst formation or morphology but caused outgrowth failure as shown in the *Pold2* KO mutants. (A) KD efficiency was confirmed by qPCR at the morula stage and blastocyst stage (2.5 and 3.5 days after microinjection respectively and 15 embryos per stage in each replicate with 3 replicates total). (B) POLD2 protein IF at blastocyst stage also confirmed the KD efficacy after *Pold2*-siRNA microinjection (number of embryos examined: Control=38, KD=36). (C, D) *Pold2* KD did not affect blastocyst morphology or formation (number of embryos examined: Control=179, KD=146). (E, F) Outgrowth failure of *Pold2* KOs can be recapitulated in *Pold2* KD embryos (number of outgrowths examined: Control=68, KD=75). The majority of KD blastocysts could not hatch from the zona pellucida. Those that did hatch resulted in abnormal growth with no obvious ICM or trophoblast cells (F, far right). Red and blue dashed lines indicate ICM outgrowth and trophoblast cells, respectively. Control: scrambled siRNA. n, number of embryos; *, $P < 0.05$. Scale bars, 100 μm.

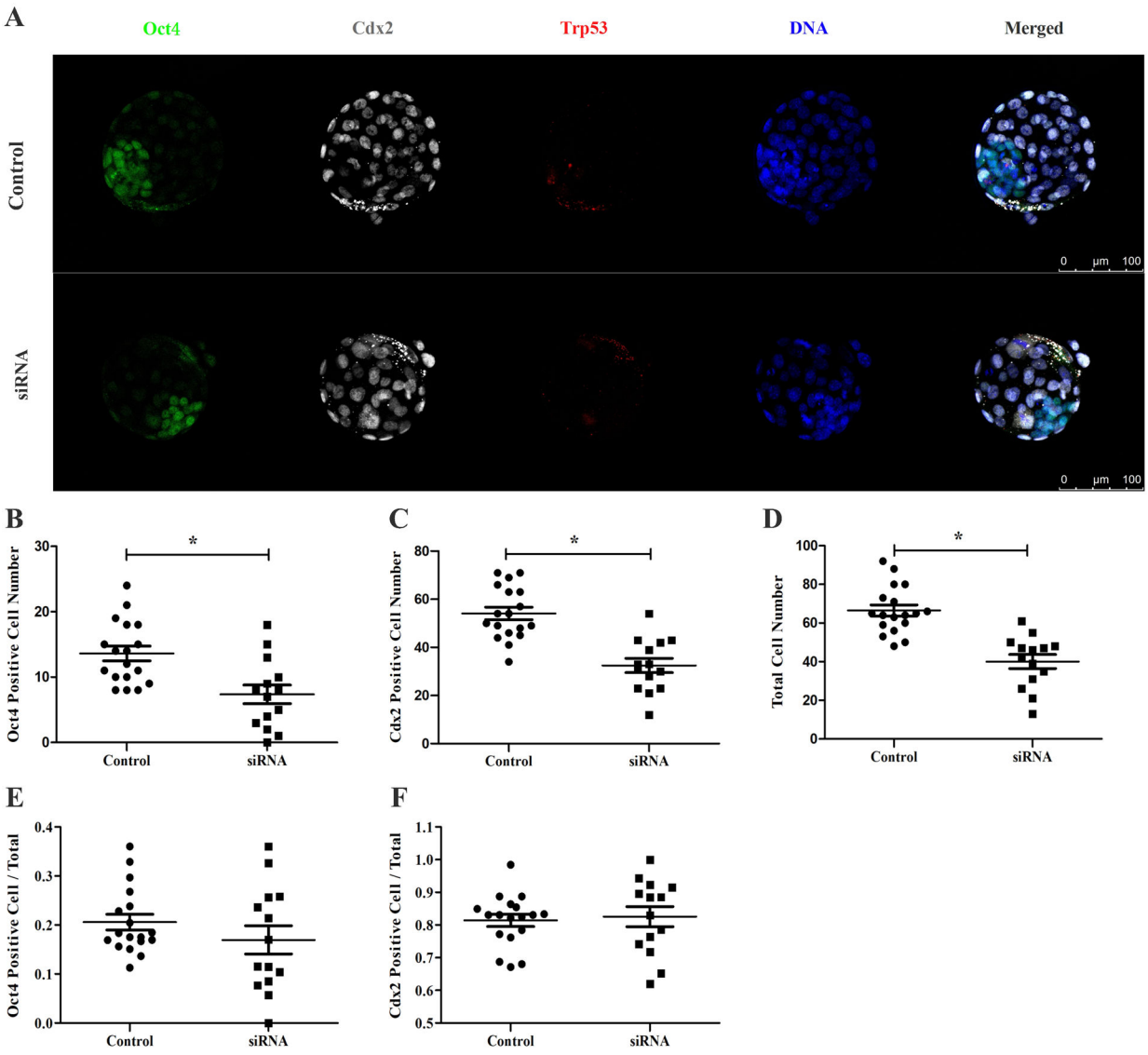

Fig. 4.

KD of *Pold2* did not affect apoptosis index or ICM/TE lineage specification. (A) IF of OCT4 (ICM marker), CDX2 (TE marker), and Ser15-phospho active TRP53 (apoptosis marker) in control and KD blastocysts (4 days after microinjection). (B, C, D) The number of OCT4 positive cells (B) and CDX2 positive cells (C) per blastocyst, as well as total cell number per blastocyst (D), were severely reduced in KD embryos. (E, F) The final percentages of OCT4 (E) and CDX2 (F) positive cells were not significantly altered between control and KD groups. Control: 18 embryos; KD: 14 embryos. *, $P < 0.05$.

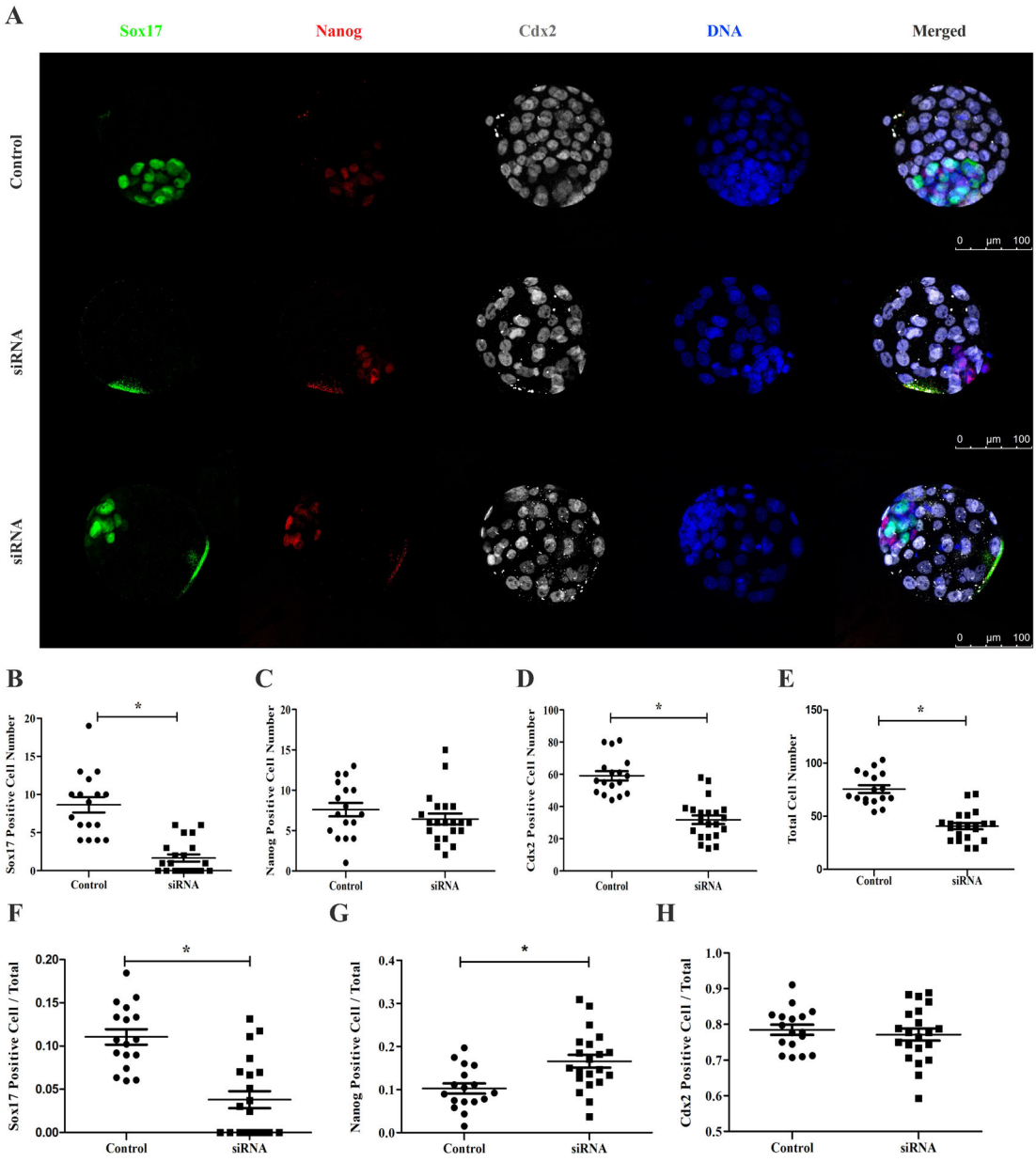

Fig. 5.

KD of *Pold2* altered PE/EPI allocation within ICM during the second lineage specification. (A) IF of SOX17 (PE marker), NANOG (EPI marker), and CDX2 (TE marker) in control and KD blastocysts (4 days after microinjection). (B, C) Although KD blastocysts contained a significantly decreased number of SOX17-positive PE cells (B), no significant change was detected on the number of NANOG-positive EPI cells (C). Significantly decreased number of CDX2-positive TE cells (D) and total cell number (E) were observed in KD embryos. The percentage of SOX17-positive PE cells (F) and NANOG-positive EPI cells (G) was significantly reduced and increased, respectively, while no change was detected on

the percentage of CDX2-positive TE cells (H). Control: 17 embryos; KD: 21 embryos. *, $P < 0.05$.